

LETTER TO THE EDITOR

## First results on Martian carbon monoxide from *Herschel*/HIFI observations<sup>★</sup>

P. Hartogh<sup>1</sup>, M. I. Błęcka<sup>2</sup>, C. Jarchow<sup>1</sup>, H. Sagawa<sup>1,3</sup>, E. Lellouch<sup>4</sup>, M. de Val-Borro<sup>1</sup>, M. Rengel<sup>1</sup>, A. S. Medvedev<sup>1</sup>, B. M. Swinyard<sup>5</sup>, R. Moreno<sup>4</sup>, T. Cavalié<sup>1</sup>, D. C. Lis<sup>6</sup>, M. Banaszkiewicz<sup>2</sup>, D. Bockelée-Morvan<sup>4</sup>, J. Crovisier<sup>4</sup>, T. Encrenaz<sup>4</sup>, M. Küppers<sup>7</sup>, L.-M. Lara<sup>8</sup>, S. Szutowicz<sup>2</sup>, B. Vandenbussche<sup>9</sup>, F. Bensch<sup>10</sup>, E. A. Bergin<sup>11</sup>, F. Billebaud<sup>12</sup>, N. Biver<sup>4</sup>, G. A. Blake<sup>6</sup>, J. A. D. L. Blommaert<sup>9</sup>, J. Cernicharo<sup>13</sup>, L. Decin<sup>9,14</sup>, P. Encrenaz<sup>15</sup>, H. Feuchtgruber<sup>16</sup>, T. Fulton<sup>17</sup>, T. de Graauw<sup>18,19,20</sup>, E. Jehin<sup>21</sup>, M. Kidger<sup>22</sup>, R. Lorente<sup>22</sup>, D. A. Naylor<sup>23</sup>, G. Portyankina<sup>24</sup>, M. Sánchez-Portal<sup>22</sup>, R. Schieder<sup>25</sup>, S. Sidher<sup>5</sup>, N. Thomas<sup>24</sup>, E. Verdugo<sup>22</sup>, C. Waelkens<sup>9</sup>, A. Lorenzani<sup>26</sup>, G. Tofani<sup>26</sup>, E. Natale<sup>26</sup>, J. Pearson<sup>27</sup>, T. Klein<sup>28</sup>, C. Leinz<sup>28</sup>, R. Güsten<sup>28</sup>, and C. Kramer<sup>25</sup>

(Affiliations are available on page 5 of the online edition)

Received 5 June 2010 / Accepted 6 July 2010

### ABSTRACT

We report on the initial analysis of *Herschel*/HIFI carbon monoxide (CO) observations of the Martian atmosphere performed between 11 and 16 April 2010. We selected the (7–6) rotational transitions of the isotopes <sup>13</sup>CO at 771 GHz and C<sup>18</sup>O and 768 GHz in order to retrieve the mean vertical profile of temperature and the mean volume mixing ratio of carbon monoxide. The derived temperature profile agrees within less than 5 K with general circulation model (GCM) predictions up to an altitude of 45 km, however, show about 12–15 K lower values at 60 km. The CO mixing ratio was determined as 980 ± 150 ppm, in agreement with the 900 ppm derived from *Herschel*/SPIRE observations in November 2009.

**Key words.** planets and satellites: atmospheres – molecular processes – radiative transfer – submillimeter: general

### 1. Introduction

Carbon monoxide was first definitely detected spectroscopically in the Martian atmosphere by Kaplan et al. (1969). From observations performed in 1967 between Mars  $L_s = 110^\circ$  and  $133^\circ$  a volume mixing ratio (vmr) of 800 ppm was deduced Kakar et al. (1977) reported the first microwave detection of CO performed in 1975, when observing the  $J = 1-0$  rotational transition during  $L_s = 339^\circ$ . They found a vmr of 1900 ppm assuming a disk-averaged continuum brightness temperature of 200 K and a constant height profile. Good & Schloerb (1981) observed the same transition in 1980 during  $L_s = 86^\circ$  and found 3200 ppm. The re-analysis of these data by Clancy & Muhleman (1983) resulted in quite different values: 800 ± 400 ppm from the Kakar et al. (1977) observation and 1400 ± 500 ppm from the Good & Schloerb (1981) observation by assuming a surface brightness temperature of 206 K, a ±10 K variation in model atmosphere temperatures, and a surface pressure of 6.5 hPa. They found 2200 ± 1000 ppm, based on their own observations of the CO (2–1) line performed in 1982 ( $L_s = 75^\circ$ ) with the same model assumptions. Clancy et al. (1990) derived a mixing ratio of 600 ± 150 ppm from 1988/9 observations ( $L_s = 197^\circ-341^\circ$ ) of the <sup>12</sup>CO and <sup>13</sup>CO transitions (1–0 and 2–1) and surface brightness temperatures between 192 and 216 K. They did not find any significant temporal variability of CO. Rosenqvist et al. (1990) found a CO vmrs between 800 and 1200 ppm depending on the

orography from Phobos/ISM observations. Lellouch et al. (1991) provided for the first time a mm-wave map of CO (1988,  $L_s = 270^\circ$ ) and deduced no significant variation from their derived value of 800 ± 200 ppm over the Mars disk. While the 230 GHz observations provided reasonable surface brightness temperatures, the values in the 115 GHz band are too high (270 K), very likely due to sideband ratio calibration errors. Billebaud et al. (1998) retrieved values between 450 and 1150 ppm from ground-based IR observations in 1990/1. Also from ground-based IR observations, Krasnopolsky (2003) found a hemispheric asymmetry with the CO vmr increasing from 850 ppm at 23° N to 1250 ppm at 50° S (at  $L_s = 112^\circ$ ). Follow-up observations of Krasnopolsky (2007) between 80° N to 75° S over 4 seasons show even larger variations between 700 and 1600 ppm. Encrenaz et al. (2006) report about a seasonal variation in CO over Hellas by a factor of 2 from 2.3 μm CO band observations by OMEGA/MEX. Infrared observations of PFS/MEX result in similar variabilities over latitude and season, i.e. with a mean value of 1100 ppm (Billebaud et al. 2009). Finally, Smith et al. (2009) derived seasonally and globally averaged 700 ppm CO vmr from CRISM/MRO observations, but with strong seasonal variations at high latitudes. The summertime near-polar CO mixing ratio was observed to fall to 200 ppm in the south and 400 ppm in the north during the time the carbon dioxide was sublimating from the seasonal ice caps.

The determination of the vertical profile of temperature and CO (together with studies of the carbon and oxygen isotopic ratios in CO) over different solar longitudes of Mars is one of the goals of the *Herschel* key programme “Water and related

<sup>★</sup> *Herschel* is an ESA space observatory with science instruments provided by European-led Principal Investigator consortia and with important participation from NASA.

chemistry in the solar system” (Hartogh et al. 2009). Here we present first results of observations performed in April 2010 around  $L_s = 76^\circ$ . In this paper we derive the CO mixing ratio and temperature profile from HIFI observations. The latter is also required for analysing other species not treated in this paper. For simplification we analyse two CO lines (the 7–6 transitions of the isotopes  $^{13}\text{CO}$  and  $\text{C}^{18}\text{O}$ ) observed at the same time and in the same sideband.

## 2. Herschel/HIFI observations

All observations were carried out in HIFI’s dual beam switch mode (de Graauw et al. 2010; Roelfsema et al. 2010) on operational days (OD) 332, 333, 334, and 337, corresponding to 11–16 April 2010 or  $L_s = 75.8^\circ$  to  $78^\circ$ . Dedicated line observations include CO (5–4, 6–5, 8–7),  $^{13}\text{CO}$  (7–6),  $\text{C}^{17}\text{O}$  (7–6), and  $\text{C}^{18}\text{O}$  (7–6). HIFI spectrometers can resolve line shapes with a spectral resolution of 140 KHz (high resolution spectrometer; HRS) or 1.1 MHz (wide band spectrometer; WBS). The integration times range from 93 s for the strongest  $^{12}\text{CO}$  lines to 9289 s for the  $\text{C}^{17}\text{O}$  observation. Numerous other CO-lines were detected in the band scans or as side products of other dedicated line observations, appearing in the intermediate frequency either in the same or other sideband (double sideband conversion), some of them with excellent signal-to-noise ratios. The first set of data was available about a week after the observations and was processed with the standard HIPE v3.0.1 modules (Ott 2010) up to level 2. This data set was not complete yet; for instance, the data of the HRS was only partly available, and pointing products therein had no entries. The flux calibration by the *Herschel* Science Centre (HSC) was still in progress and some calibration errors occurred in this first data set. Furthermore, it turned out in the band scan data that the line amplitudes of the detected CO lines were not always exactly the same in the upper and lower sidebands. Last but not least, the HIFI spectra suffered from a relatively large baseline ripple (Fig. 1). Fortunately, the frequency of the ripple generally is the same in the vertical and horizontal polarizations; however, phase and amplitudes are different so they need a dedicated treatment before both polarizations can be averaged. Solutions of these problems are under way, but only partly available now. Therefore we decided to analyse the data with the following boundary conditions: (i) line-to-continuum ratio rather than absolute fluxes (requires assumptions on the surface brightness); (ii) only horizontal polarization (hence decreases the signal-to-noise ratio); (iii) only lines in the same sideband; (iv) only WBS spectra. The surface pressure averaged over the visible Mars disk changes diurnally in the order of 10% (derived from the European Mars Climate Data Base, EMCD v4.1, Forget et al. 1999; Lewis et al. 1999 and our own general circulation model, Hartogh et al. 2005; Medvedev & Hartogh 2007). Therefore we introduced boundary condition; (v) to analyse only lines observed at the same time. The only data that fulfil these criteria are the (7–6) transitions of  $^{13}\text{CO}$  and  $\text{C}^{18}\text{O}$ , which were observed on 13 April 2010 at 05:33 UT (Obs. Id. 1342194686). The integration time for this observation was 900 s.

## 3. Analysis and discussion

Compared to cometary observations of HIFI (Hartogh et al. 2010; de Val-Borro et al. 2010), the baseline ripple on the Mars observations is rather large because of its strong continuum emission. This phenomenon was frequently observed by ground-based observations of planets. While in the cometary case, the

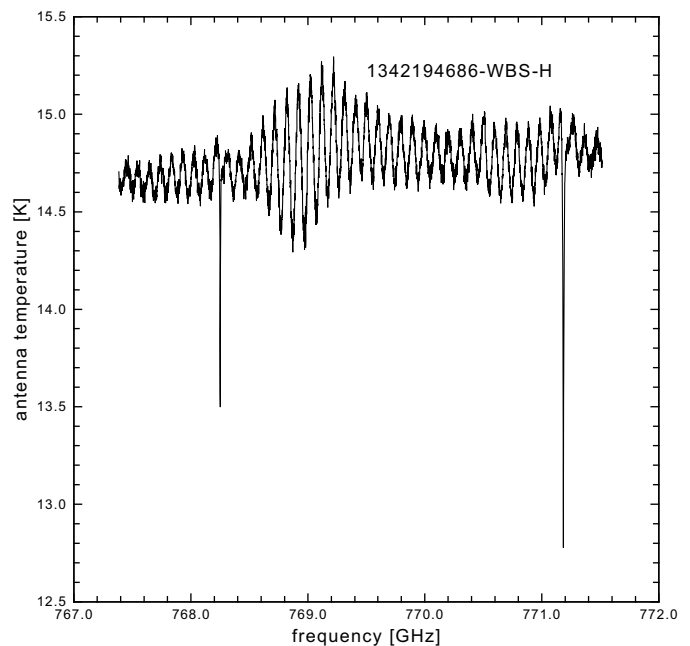


**Fig. 1.**  $\text{C}^{18}\text{O}$  (left) and  $^{13}\text{CO}$  (right) WBS spectra before baseline ripple removal. Both lines are in the same sideband.

baseline ripple has been removed with a polynomial fit, for Mars we determined the baseline frequencies by a normalized periodogram according to Lomb (1976) and subtracted 3 periods from the original spectrum. The influence of the line shapes on the determination of the baseline periods is negligible when taking the large number of periods in the spectrum into account. The observed spectral lines have been modelled using a standard radiative transfer code: Mars was assumed as a perfect sphere surrounded by a set of hundred concentric atmospheric layers of 1 km thickness each (as in Rengel et al. 2008). Within each layer the atmospheric temperature, pressure, and volume-mixing ratio of carbon monoxide have been assumed constant. The surface continuum emission was modelled as blackbody emission using a temperature distribution falling off towards the edge of the apparent disk according to  $T(\alpha) = T_0 \times (1 - 0.2 \times (1 - \cos(\alpha)))$ , with  $\alpha$  running from  $0^\circ$  (nadir) to  $90^\circ$  (limb) across the apparent disk (limb darkening, compare also Cavalié et al. 2008).

The emission was obtained by integrating over the apparent disk using 64 concentric rings distributed unevenly over the disk and the limb region. The variation in the path lengths through the atmosphere were taken into account fully when calculating the radiation transfer for each ring. In our model the total continuum flux emitted by the surface depends purely on the choice of the temperature  $T_0$ , which defines the temperature scale for the temperature profile to be retrieved. We have adjusted  $T_0$  in such a way as to exactly match the total flux predicted by the “Mars continuum model” of  $\sim 4230$  Jy provided by Lellouch & Amri (2008) and to match the temperature fall off towards the limb therein by a factor 0.2. The error of the modelled flux is 5%.

Absorption coefficients for the CO spectral lines were calculated using the HITRAN 2008 spectral line catalogue, keeping the terrestrial isotopic ratios in it; i.e.,  $\text{C}^{16}\text{O}/\text{C}^{18}\text{O} = 498.70$  and  $^{12}\text{CO}/^{13}\text{CO} = 89.01$ . Krasnopolsky et al. (2007) conclude that the deviations of these isotopic ratios on Mars compared to Earth are less than 2%. However, to account for carbon dioxide instead of air as broadening gas, the broadening parameters provided by the catalogue were multiplied by a factor of 1.4 according to Nakazawa & Tanaka (1982).

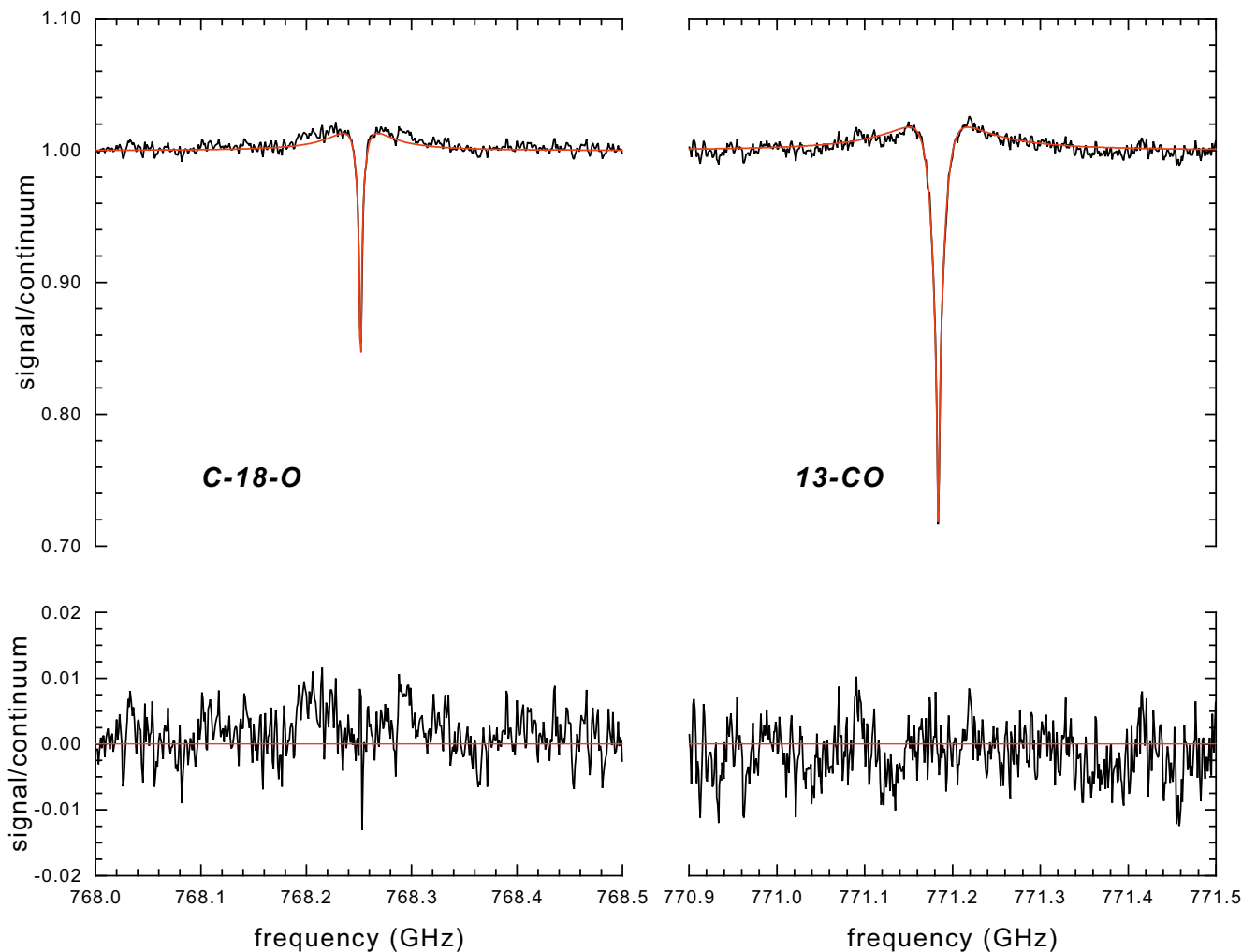


**Fig. 2.** The  $^{13}\text{CO}$  and  $\text{C}^{18}\text{O}$  lines after removal of the baseline ripples. A radiative transfer model was fitted simultaneously to the spectra to retrieve temperature profile and volume mixing ratio of CO. The lower panels show the differences between model and observations.

To obtain a temperature profile and the mixing ratio of CO we employed Rodgers’s optimal estimation method (Rodgers 1976, 1990). This method uses so-called “a priori” information – in our case the best estimate of the temperature profile and CO mixing ratio profile – which is then updated to allow for a best fit of the spectral line shapes (minimization of  $\chi^2$ ). This a priori profile was taken from our MAOAM general circulation model (Hartogh et al. 2005) considering the exact observation date, geometry, and time of the HIFI observations. The surface pressure averaged over the visible disk was 6.7 hPa. Compared to temperature profiles derived from the EMCD, we find temperature differences less than 3 K between 3–60 km. EMCD provides about 5 K higher temperatures below 3 km and 3 to 5 K higher temperatures between 60–80 km. Up to 100 km, both models slowly merge to almost the same temperature. It is worth noting a high degree of coincidence of the averaged temperature profiles over the field of view of the telescope with the two models. Even though the one from EMCD represents monthly averaged fields, the one from MAOAM is based on an instantaneous snapshot, and generally the altitude-latitude distributions differ. This increases our degree of confidence in the simulated temperatures.

A simultaneous fit of the two spectral lines allows retrieving temperature and mixing ratios independently, because of the rather different optical depth of the two lines, where the  $^{13}\text{CO}$  line is optically thick ( $\tau = 6.3$  in line centre) and the

$\text{C}^{18}\text{O}$  line being optically thin ( $\tau = 1.1$ ). Figure 2 shows the simultaneously fitted spectra of  $^{13}\text{CO}$  and  $\text{C}^{18}\text{O}$  (and the residuals) after the removal of the baseline ripple. The retrieved CO mixing ratio amounts to  $980 \pm 100$  ppm which is in agreement with the one detected by SPIRE observations during  $L_s = 5^\circ$  from 6 November 2009 at 20:20 UT (Swinyard et al. 2010) under rather similar surface pressure conditions. The SPIRE value of 900 ppm has been used as an a priori input to the retrieval algorithm. Figure 3 shows the corresponding temperature profile and the averaging kernels. The latter provide information about the sensitivity of the retrieval versus altitude. Although the contribution of the a priori profile to the retrieved temperature profile is less than 10% below 60 km, it fits quite well to the profiles predicted by the GCMs. However, the differences are least with EMCD near the ground ( $\sim 5$  K) and with MAOAM near 60–70 km. Nevertheless, the observations provide about 12–15 K lower temperatures near 65 km. The temperature inversion between 40–60 km predicted by the GCMs should be manifested in an emission feature in the centre of the CO lines, which obviously is not the case. The 5% error of the model continuum flux translates into a roughly 10 K shift of the temperature profiles, i.e., all temperatures will be about 10 K higher or lower than the retrieved value. In the first case, the agreement with the model profile is better between 40–80 km (although still without temperature inversion) but worse below 40 km. In the second case the agreement is worse for all altitudes.

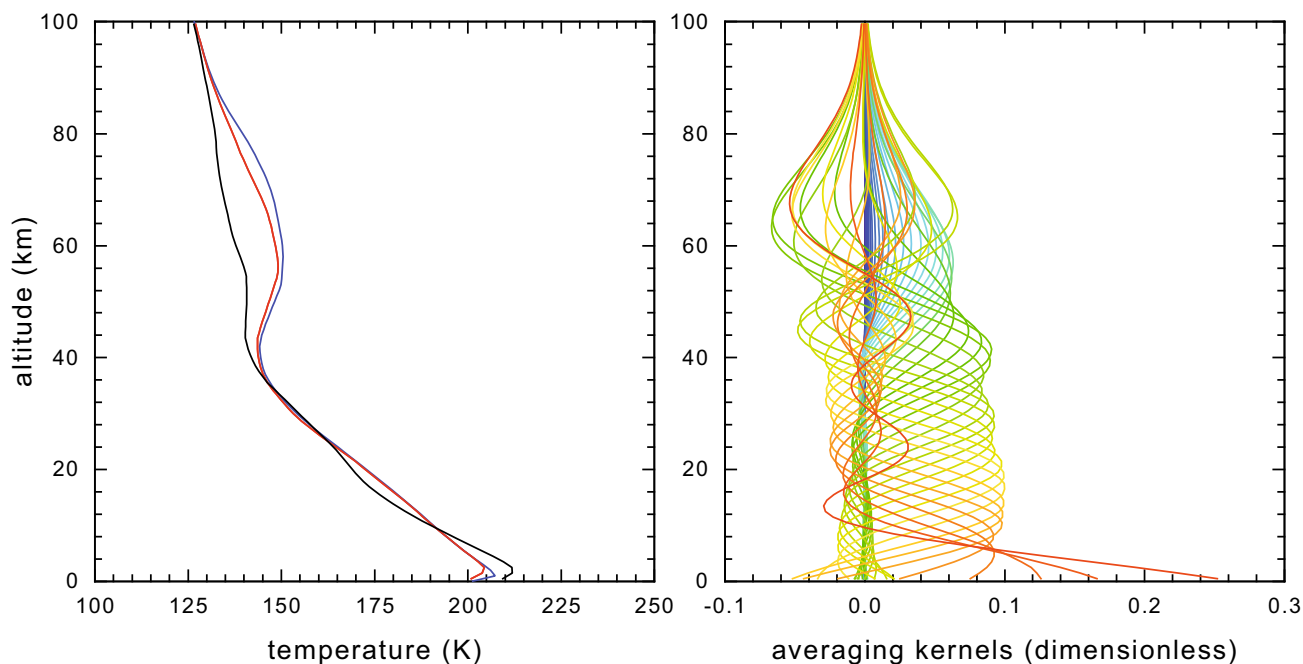


**Fig. 3.** Retrieved vertical profile of temperature (*left*) and averaging kernels (*right*). The averaging kernels express the response of the fitted temperature profile to a delta function perturbation in the true profile at a certain altitude (see [Rodgers 1990](#), for a sound introduction of this quantity). Different colours are used to distinguish the averaging kernels belonging to perturbations at the different altitude levels. The blue temperature profile is derived from EMCD.

#### 4. Summary

This work presents the first simultaneous retrievals of temperature and carbon monoxide in the Martian atmosphere derived from HIFI data. The temperature profile can be used as an input parameter for determining of concentrations of other gases observed by HIFI during the same period. Future work will include all observed CO transitions in order to better constrain the temperature profile above 60 km and take advantage of the much wider opacity range for retrieving the vertical profile of CO.

*Acknowledgements.* HIFI has been designed and built by a consortium of institutes and university departments from across Europe, Canada, and the United States under the leadership of SRON Netherlands Institute for Space Research, Groningen, The Netherlands, and with major contributions from Germany, France, and the US. Consortium members are: Canada: CSA, U. Waterloo; France: CESR, LAB, LERMA, IRAM; Germany: KOSMA, MPIfR, MPS; Ireland: NUI Maynooth; Italy: ASI, IFSI-INAF, Osservatorio Astrofisico di Arcetri-INAF; Netherlands: SRON, TUD; Poland: CAMK, CBK; Spain: Observatorio Astronómico Nacional (IGN), Centro de Astrobiología (CSIC-INTA). Sweden: Chalmers University of Technology – MC2, RSS & GARD; Onsala Space Observatory; Swedish National Space Board, Stockholm University – Stockholm Observatory; Switzerland: ETH Zürich, FHNW; USA: Caltech, JPL, NHSC. HIPE is a joint development by the *Herschel* Science Ground Segment Consortium, consisting of ESA, the NASA *Herschel* Science Center, and the HIFI, PACS and SPIRE consortia. This development has been supported by national funding agencies: CEA, CNES, CNRS (France); ASI (Italy); DLR (Germany). Additional funding support for some instrument activities has been provided by ESA. Support for this work was provided by NASA through an award issued by JPL/Caltech. MIB, MB, and SS are supported by the Polish Ministry of Education and Science (MNiSW). DCL is supported by the NSF, award AST-0540882 to the Caltech Submillimeter Observatory.

#### References

Billebaud, F., Rosenqvist, J., Lellouch, E., et al. 1998, *A&A*, 333, 1092  
 Billebaud, F., Brillet, J., Lellouch, E., et al. 2009, *Planet. Space Sci.*, 57, 1446

Cavalié, T., Billebaud, F., Encrenaz, T., et al. 2008, *A&A*, 489, 795  
 Clancy, R. T., & Muhleman, D. O. 1983, *ApJ*, 273, 829  
 Clancy, R. T., Muhleman, D. O., & Berge, G. L. 1990, *J. Geophys. Res.*, 95, 14543  
 de Graauw, Th., Helmich, F. P., Philipps, T. G., et al. 2010, *A&A*, 518, L6  
 de Val-Borro, M., Hartogh, P., Crovisier, J., et al. 2010, *A&A*, 521, L50  
 Encrenaz, T., Fouchet, T., Melchiorri, R., et al. 2006, *A&A*, 459, 265  
 Forget, F., Hourdin, F., Fournier, R., et al. 1999, *J. Geophys. Res.*, 104, 24155  
 Good, J., & Schloerb, F. P. 1981, *Icarus*, 47, 166  
 Hartogh, P., Crovisier, J., de Val-Borro, M., et al. 2010, *A&A*, 518, L150  
 Hartogh, P., Lellouch, E., Crovisier, J., et al. 2009, *Planet. Space Sci.*, 57, 1596  
 Hartogh, P., Medvedev, A. S., Kuroda, T., et al. 2005, *JGR*, 110, 11008  
 Kakar, R. K., Walters, J. W., & Wilson, W. J. 1977, *Science*, 196, 1090  
 Kaplan, L. D., Connes, J., & Connes, P. 1969, *ApJ*, 157, L187  
 Krasnopolsky, V. A. 2003, *Icarus*, 165, 315  
 Krasnopolsky, V. A. 2007, *Icarus*, 190, 93  
 Krasnopolsky, V. A., Maillard, J. P., Owen, T. C., Toth, R. A., & Smith, M. D. 2007, *Icarus*, 192, 396  
 Lellouch, E., & Amri, H. 2008, <http://www.lesia.obspm.fr/perso/emmanuel-lellouch/mars/>  
 Lellouch, E., Paubert, G., & Encrenaz, T. 1991, *Planet. Space Sci.*, 39, 219  
 Lewis, S. R., Collins, M., Read, P. L., et al. 1999, *J. Geophys. Res.*, 104, 24177  
 Lomb, N. R. 1976, *Ap&SS*, 39, 447  
 Medvedev, A. S., & Hartogh, P. 2007, *Icarus*, 186, 97  
 Nakazawa, T., & Tanaka, M. 1982, *J. Quant. Spec. Rad. Trans.*, 28, 409  
 Ott, S. 2010, *Astronomical Data Analysis Software and Systems XIX*, ed. Y. Mizumoto, K.-I. Morita, & M. Ohishi, *ASP Conf. Ser.*, in press  
 Rengel, M., Hartogh, P., & Jarchow, C. 2008, *Planet. Space Sci.*, 56, 1368  
 Rodgers, C. D. 1976, *Rev. Geophys.*, 14, 609  
 Rodgers, C. D. 1990, *J. Geophys. Res.*, 95, 5587  
 Roelfsema, P. R., Helmich, F. P., Teyssier, D., et al. 2010, *A&A*, submitted  
 Rosenqvist, J., Bibring, J., Combes, M., et al. 1990, *A&A*, 231, L29  
 Smith, M. D., Wolff, M. J., Clancy, R. T., & Murchie, S. L. 2009, *J. Geophys. Res. (Planets)*, 114, 0  
 Swinyard, B. M., Hartogh, P., Sidher, S., et al. 2010, *A&A*, 518, L151

- 
- <sup>1</sup> Max-Planck-Institut für Sonnensystemforschung, 37191 Katlenburg-Lindau, Germany
- <sup>2</sup> Space Research Centre, Polish Academy of Sciences, Warsaw, Poland
- <sup>3</sup> Environmental Sensing & Network Group, NICT, 4-2-1 Nukui-kita, Koganei, Tokyo 184-8795, Japan
- <sup>4</sup> LESIA, Observatoire de Paris, 5 place Jules Janssen, 92195 Meudon, France
- <sup>5</sup> STFC Rutherford Appleton Laboratory, Harwell Innovation Campus, Didcot, OX11 0QX, UK
- <sup>6</sup> California Institute of Technology, Pasadena, CA 91125, USA
- <sup>7</sup> Rosetta Science Operations Centre, European Space Astronomy Centre, European Space Agency, Spain
- <sup>8</sup> Instituto de Astrofísica de Andalucía (CSIC), Spain
- <sup>9</sup> Instituut voor Sterrenkunde, Katholieke Universiteit Leuven, Belgium
- <sup>10</sup> DLR, German Aerospace Centre, Bonn-Oberkassel, Germany
- <sup>11</sup> Astronomy Department, University of Michigan, USA
- <sup>12</sup> Université de Bordeaux, Laboratoire d'Astrophysique de Bordeaux, France
- <sup>13</sup> Laboratory of Molecular Astrophysics, CAB-CSIC, INTA, Spain
- <sup>14</sup> Sterrenkundig Instituut Anton Pannekoek, University of Amsterdam, Science Park 904, 1098 Amsterdam, The Netherlands
- <sup>15</sup> LERMA, Observatoire de Paris, France
- <sup>16</sup> Max-Planck-Institut für extraterrestrische Physik, Giessenbachstraße, 85748 Garching, Germany
- <sup>17</sup> Bluesky Spectroscopy, Lethbridge, Canada
- <sup>18</sup> SRON Netherlands Institute for Space Research, Landleven 12, 9747 AD, Groningen, The Netherlands
- <sup>19</sup> Leiden Observatory, University of Leiden, The Netherlands
- <sup>20</sup> Joint ALMA Observatory, Chile
- <sup>21</sup> Institute d'Astrophysique et de Géophysique, Université de Liège, Belgium
- <sup>22</sup> *Herschel* Science Centre, European Space Astronomy Centre, European Space Agency, Spain
- <sup>23</sup> Department of Physics and Astronomy, University of Lethbridge, Canada
- <sup>24</sup> Physikalisches Institut, University of Bern, Switzerland
- <sup>25</sup> KOSMA, I. Physik. Institut, Universität zu Köln, Zùlpicher Str. 77, D 50937 Köln, Germany
- <sup>26</sup> Osservatorio Astrofisico di Arcetri-INAF, Largo E. Fermi 5, 50100 Florence, Italy
- <sup>27</sup> Jet Propulsion Laboratory, Caltech, Pasadena, CA 91109, USA
- <sup>28</sup> Max-Planck-Institut für Radioastronomie, Auf dem Hügel 69, D53121 Bonn Germany